Catal Lett (2012) 142:1344–1351
DOI 10.1007/s10562-012-0895-0

Polyaniline-Supported Atomic Gold Electrodes: Comparison with Macro Electrodes

Ilana Schwartz · Alex P. Jonke · Mira Josowicz · Jiří Janata

Received: 16 July 2012 / Accepted: 16 August 2012 / Published online: 11 September 2012

Abstract Under precisely controlled conditions, atomic gold electrodes with even or odd number of Au atoms per polyaniline repeat unit (Pt/PANI/Au_N for $0 < N < 7$) were prepared. The electrochemical behavior of these new electrodes is compared with that of macro gold and PANI coated platinum electrodes by testing electrochemical oxidation of *n*-propanol and *iso*-propanol. This study allowed us to separate the behavior dominated by that of macroscopic gold in strongly alkaline medium and by that of the quantized odd–even effect of atomic gold. Within this overarching scope, there is a specific oxidation pattern attributable to the structural differences between the two isomers of propanol. The significance of this research lies in the recognition of high specific catalytic activity of atomic gold, which is at least three orders of magnitude higher than that of bulk gold for the oxidation of alcohols. It points to a substantial saving of the precious metal without the loss of catalytic activity, which is important in fuel cells and in other energy conversion device applications.

Keywords Atomic metals · Odd–even pattern · Propanol electrooxidation · Gold electrodes

Electronic supplementary material The online version of this article (doi:10.1007/s10562-012-0895-0) contains supplementary material, which is available to authorized users.

I. Schwartz · A. P. Jonke · M. Josowicz · J. Janata (✉)
School of Chemistry, Georgia Institute of Technology, Atlanta, GA 30332-0400, USA
e-mail: jiri.janata@chemistry.gatech.edu

1 Introduction

Interest in the electro catalytic oxidation of alcohols has increased greatly due to their potential application in fuel cells [1–3]. This oxidation can be catalyzed by a variety of metals, two of the most active being platinum and gold [3–7]. These metals can either be used in polycrystalline form or as large, polydispersed cluster aggregates containing millions of metal atoms. The aim of this paper is to compare electrochemical behavior of polycrystalline gold electrodes, polycrystalline platinum electrodes, and Pt electrodes coated with polyaniline containing defined atomic Au particles (Pt/PANI/Au_N with $N = 2$–7). The electrochemistry of electrodes with $N = 1$ was indistinguishable from that of $N = 0$.

Polyaniline polymerized from an acidic medium has been used as a support matrix for the insertion of metal clusters [8, 9]. It is a stable conjugated polymer, which is unique due to its ionic and electronic conductivity [10, 11]. Electro polymerization of aniline is done typically in acidic medium and results in the protonated emeraldine (semiquinone) form of PANI. The protonated imine functionality of the PANI has a strong affinity for certain complexed metal anions. In this paper we utilized the strong complexation of $AuCl_4^-$ for step-wise insertion of Au clusters into the PANI matrix [12]. This redox-driven process can occur spontaneously, just by dipping the platinum coated with polyaniline (Pt/PANI) electrode into the solution containing $AuCl_4^-$, resulting in polydispersed gold clusters, imbedded in the PANI matrix. In this reaction, PANI in its emeraldine form acts as a reducing agent, which reduces $AuCl_4^-$ to metallic gold clusters of various sizes. Only a limited control over the size of the inserted Au particles can be achieved by selection of experimental conditions during this "top–down" deposition [13]. On the

other hand, in the precisely controlled "bottom–up" deposition process, metal is inserted in a step-wise atom-by-atom, defined deposition cycles [14]. The discussion of this process and the experimental proofs of controlled atomic size are also included in the original paper [14].

The key point is the size control by the stoichiometry of the PANI*$AuCl_4^-$ complex formation, while the spontaneous reduction is suppressed by precise and synchronized potential control. The result is a PANI matrix containing Au_N clusters with $N = 0$ and 2–7. The electrochemical behavior of the electrodes followed the predicted odd–even pattern of the fluctuation of the HOMO/LUMO gap energy [14].

Electrochemical oxidation of *n*-propanol (*n*-PrOH) and of *iso*-propanol (*i*-PrOH) in 1 M KOH has been used as the probing reaction in order to demonstrate the electrochemical efficiency of various forms of gold. The details of the alcohol oxidation, identification of the oxidation products, the effect of carbonate, and the effect of the kind and concentration of hydroxide have not been investigated. All experiments were done in the presence of oxygen, unless stated otherwise. In order to aid visual comparison between different kinds of electrodes, the concentration of propanol in 1 M KOH solution was kept constant at 0.5 M. Due to the fact that adsorption of organic molecules onto platinum is often irreversible while adsorption onto gold is reversible, the catalytic poisoning effects seen for Pt are not seen for gold [7].

For electro catalytic oxidation of alcohols on gold, the rate determining step is the cleavage of the C–H_α bond [3].

$$H_\alpha R{-}OH \leftrightarrows H_\alpha R{-}O^- + H^+$$

The deprotonation of the alcohol occurs at high pH, and it is dependent on the pK_a of the alcohol. Once deprotonated, the reactivity of the alkoxide intermediate, $H_\alpha R{-}O^-$, depends on the state of the electrode material being able to abstract the H_α. For primary alcohol (e.g. *n*-PrOH) the alkoxide is more active towards the electrochemical oxidation leading to propionic aldehyde, which can be further oxidized, while for the secondary alcohols (e.g. *i*-PrOH) the final product is the corresponding ketone (e.g. acetone).

$$H_\alpha R{-}O^- \leftrightarrows R{=}O + H_\alpha{}^+ + 2e^-$$

Aldehydes are unstable in alkaline solutions, and in the presence of oxygen, decompose to a variety of products or react quickly with other acceptors [15].

The main objective of our work was to contrast the electrochemical behavior of polyaniline supported atomic gold electrodes with that of the bulk Au electrode. Besides the odd–even pattern reported earlier, [14] there are unique aspects of atomic gold electrodes (AGE) that are highlighted by differences in oxidation of *n*-PrOH and *i*-PrOH, respectively.

2 Experimental Section

2.1 Chemicals

The following compounds, all ACS grade, were used during experimentation: HBF_4 (48 %) from Alfa Aesar, aniline (99.5 %), *n*-propanol from Sigma Aldrich, KOH from EMD, and *iso*-propanol from J.T. Baker.

2.2 Electrochemical Cell Set-up and Methods

A standard three-electrode cell and CHI 660 potentiostat (CH Instrument, Inc) were used in all electrochemical experiments. As working electrodes (WE), platinum or gold disk electrodes, both with diameter of 1.2 mm ($A = 1.13 \times 10^{-3} cm^2$) from Bioanalytical Systems (BAS) were used. For preparation of the atomic gold electrodes (AGE), platinum electrodes deposited on quartz crystals ($A = 0.236\ cm^2$) obtained from International Crystals were used. The procedure for the preparation of the defined atomic gold aggregates in polyaniline films deposited on platinum crystals Pt/PANI/$Au_{(N=2-7)}$ was described previously [14].

The counter electrode (CE) was platinum foil. The reference electrode (REF) was Ag/AgCl in 1 M KCl//1 M KNO_3. The double-junction in the reference electrode was used in order to prevent contamination of 1 M KOH solution with chloride ion. All potentials reported in this study are referred to this electrode ($E = +236$ mV versus SHE). The cyclic voltammograms (CVs) were recorded with a scan rate of 50 mV s^{-1}, unless stated otherwise. Prior to their use, platinum and gold (BAS) electrodes were polished with Buehler micro polish II Al_2O_3 0.05 microns and sonicated in water for 6 min. If mechanical polishing was not adequate, the electrodes were polished electrochemically in 1 M H_2SO_4 by taking 10 CVs with a scan rate of 1 V s^{-1} followed by taking 6 CVs with a scan rate of 0.05 V s^{-1}. The CVs were always initiated from open cell potential and recorded within the potential range from -0.7 to 0.55 V for the BAS electrodes and -0.6 to 0.45 V for the Pt electrode deposited on quartz crystal.

3 Results

3.1 Odd–Even Electrochemistry

The polyaniline matrix is a necessary component of the AGE electrodes. In 1 M KOH solution Pt electrode coated with PANI has its own electrochemical background signature that resembles the CV of the Pt-bulk electrode (Fig. 1). In that figure are shown also representative examples of CVs corresponding to gold oxide formation and reduction for even

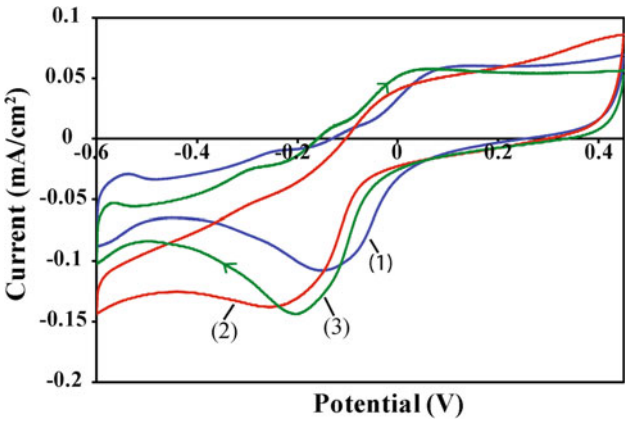

Fig. 1 Steady-state cyclic voltammograms for (1) Pt/PANI, (2) Pt/PANI/Au_4, and (3) Pt/PANI/Au_5

number of gold ($PANIAu_4$) and odd number of gold ($PANIAu_5$) in PANI. The reduction of gold oxide in PANI is taking place in the range from −180 to − 260 mV. Peak potentials corresponding to the reduction of gold oxide at AGEs correspond to that of the bulk gold electrode [16]. The hints of step-wise Au oxidation are seen only for the AGEs containing odd-number of Au atoms.

Oxidation of *n*-PrOH and *i*-PrOH in 1 M KOH on solid polycrystalline Au electrode is used as the benchmark. Since voltammograms for both alcohols contain the same features, we show only the CVs for *n*-PrOH (Fig. 2). Its oxidation potential peak at +0.240 V belongs to oxidation of chemisorbed alkoxide on the Au surface covered with adsorbed OH^- ions. Formation of gold oxide at potentials more positive, progressively blocks this reaction. The peak oxidation current is increasing with the increasing number of cycles until it reaches a stable state [17]. This feature will be discussed in greater detail later. On the reverse sweep, a new oxidation peak at +0.08 V appears that is attributed to the removal of the blocking species produced in the forward scan [18]. Note the progressive increase of both peaks upon cycling, highlighted by the upward pointing arrow.

Oxidation of both propanols on AGEs is surveyed in Fig. 3. The first peak (I) located between −0.1 and −0.2 V coincides with the oxidation of propanol on Pt electrode coated with polyaniline (Pt/PANI/$Au_{N=0}$), as shown in the inserts to Fig. 3. It is necessary to point out, that while there is only a limited oxidation of propanol on bare Pt electrode, PANI coating makes it possible. When oxidation of *n*-PrOH is taking place at Pt/PANI/$Au_{N=0}$, oxidation peaks at −0.09 V in a forward scan, and at −0.30 V on the reverse scan, are seen. In contrast, for i-PrOH only oxidation peak in the forward scan, at −0.13 V, is seen. Furthermore, for both alcohols, the magnitude of this oxidation peak current at the forward scan remains the same and it is accompanied by a reduction peak at approx. −0.13 V (see Fig. 3a, b inserts).

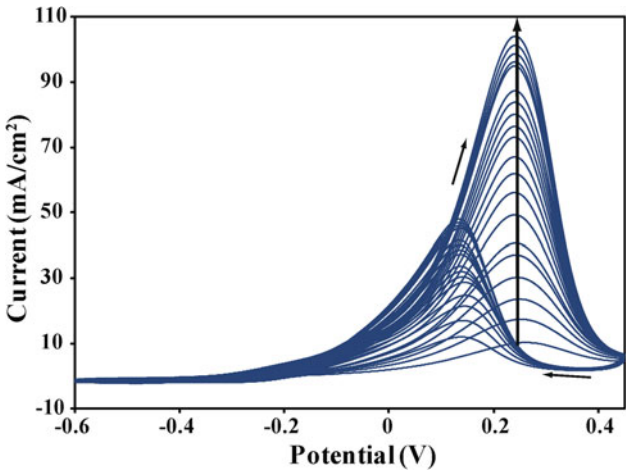

Fig. 2 Oxidation of 0.5 M *n*-PrOH, in 1 M KOH recorded at polycrystalline Au electrode (BAS). Note the progressive increase of the magnitude of the peak currents, indicated by the *vertical arrows*

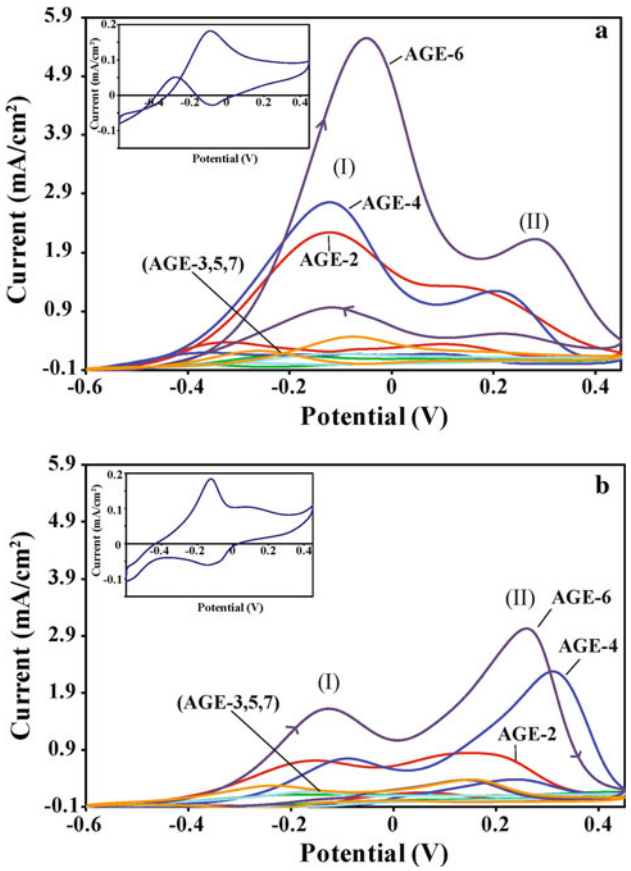

Fig. 3 Survey of the steady-state CVs for oxidation of **a** *n*-PrOH and **b** *i*-PrOH for Pt/PANI/Au_N ($2 < N < 7$) electrodes. The *insets* in both *panels* correspond to $N = 0$. The *insets* are shown at 100 × greater magnification in order to more clearly display their features. The numbering of the individual CVs corresponds to the number of inserted Au atoms. Cyclic voltammograms for odd-numbered Au atoms are shown as a *(3,5,7)* group

Significant differences between voltammograms recorded for PANI/$Au_{(N=2-7)}$ in Fig. 3a for oxidation of *n*-PrOH and Fig. 3b for oxidation of *i*-PrOH, are evident. The magnitude of the peak (I) current is significantly smaller for *i*-PrOH when compared to *n*-PrOH for the same Au_N. The opposite applies to the peak (II) that is located between 0.2 and 0.4 V. The magnitude of both peaks somewhat increases in the presence of oxygen, but it is not completely eliminated by the deaeration of the sample. In other words, while the mediated oxidation by $OH^{\cdot}$ appears to be responsible for peak I, that species is not generated exclusively by the reduction of oxygen. The absence of that peak at solid gold electrode (Fig. 2) is a strong indication that Pt must be present for the peak I (at −0.2 V) to appear. The peak II (at +0.2 V) is due to the direct oxidation of propanols on Au particles and shows the strong odd–even effect.

In order to obtain more information about the influence of the gold atomic size and its arrangement, the results have been summarized and compared to the solid gold electrode. There are several remarkable differences in these voltammograms (Fig. 3); first, there are two oxidation peaks seen on the forward scan and two oxidation peaks on the reverse scan. They are best identified on CV for AGE-6. Second, the position of the oxidation peaks (I) and (II) does depend on the N-number of Au atomic agglomerates in the PANI. The corresponding peaks are clearly separated, by as much as 320 mV for AGE-2, AGE-4, and AGE-6. Third, the dominating "odd–even" activity pattern as reported previously, [14] is clearly visible. The different magnitudes of peak (I) and peak (II) currents as well as the peak potentials separations for *n*-PrOH and *iso*-PrOH clearly indicate different electrode kinetics and different oxidation mechanisms. They will be subject to further studies.

3.2 Dependence on the Scan Rate

Peak current i_p for oxidation of *n*-PrOH at Au bulk electrodes has shown linear dependence on the square root of the scan rate, $v^{1/2}$, up to 100 mV s^{-1}, but at higher scan rates, the i_p decreased [19]. That behavior has been attributed to the slow, irreversible charge transfer coupled with adsorption. A similar scan rate behavior has been found at AGEs, but with some differences depending on the *N*-number of gold atoms. The representative plots of i_p vs $v^{1/2}$ show linear behavior for the oxidation of *n*-PrOH at PANI/Au_6, with the slope for peak I being 3.8 times higher than for peak II. On the other hand, the scan rate dependence for oxidation of *i*-PrOH at PANI/Au_6 is non-linear for both peaks, and has approximately the same non-linear trend for the peak I and peak II (Fig. 4). At PANI/Au_5 electrodes (not shown), the peak currents are approximately 20× lower, due to the odd–even effect, but are

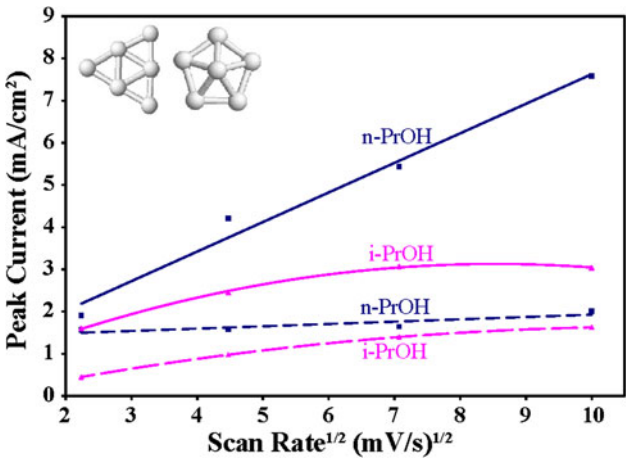

Fig. 4 Dependence of peak current on square root of scan rate for Pt/PANI/Au_6 for both alcohols. The range of examined scan rates is from 5 to 100 mV s^{-1}. The *solid lines* correspond to peak I, and the *dashed lines* to peak II. The icons show the calculated highest probability of the shape of the Au_6 clusters [20, 21]

linear for both alcohols. That could be explained by much lower rate of electron transfer relative to the mass transport and relative to the rate of desorption of the product. The icons representing the calculated [20, 21] highest binding energy (i.e. highest stability) shapes for Au_6 isomers are included.

3.3 Electrode Activation

The change of activity of polycrystalline Au electrode upon oxidation of propanol in 1 M KOH is shown in Fig. 5. In that experiment, the cycling was interrupted after approximately first 20 cycles (Fig. 5a, point A). After thorough rinsing, the electrode was stored in D.I. water for 10 min and the cycling in propanol resumed. Both peaks grew again (Fig. 5b, point B to point C), but both reached a slightly lower steady state. After another 10 min interruption and storage in D.I. water, the third set was recorded (Fig. 5c) The peaks grew again from point D to E, but ended in a lower steady state yet. After that the electrode was cycled in 2.5 mM Ru(II)/(III) hexamine in 1 M KNO_3. Cycling of the electrode in this redox couple showed a "normal" cyclic behavior, i.e. steady decrease within the first 5 cycles until reaching steady state due to formation of a depletion layer [22]. Immediately after the Ruhex treatment, the same Au electrode resumed the "activation" behavior in oxidation of propanol (Fig. 5d, points F to G). The possible explanation of this behavior is as follows. Oxidation of propanol at Au electrodes in alkaline medium proceeds through formation of $OH^{\cdot}$ radical as an intermediate [19]. It is possible that this species activates the electrode by increasing the number of active sites. That

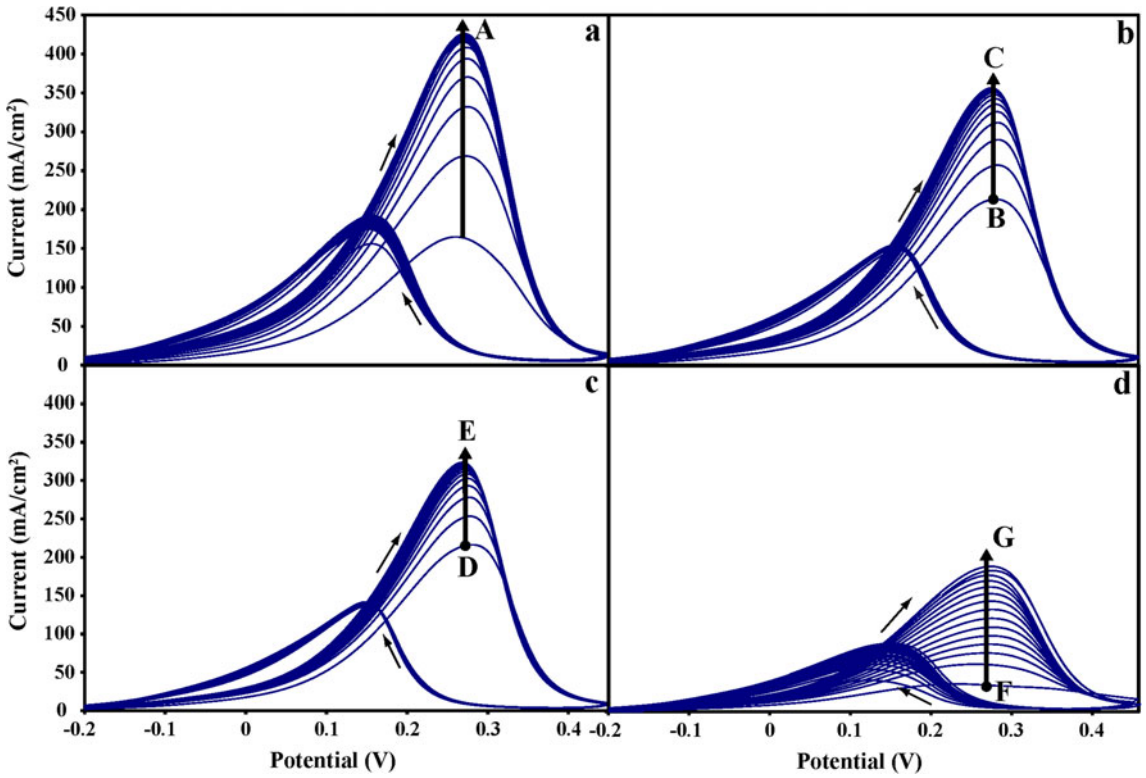

Fig. 5 The activation pattern of polycrystalline Au electrode (BAS). The *arrows* again indicate the changes from scan 1 to 20. For explanation of the experimental sequence, please see the text

mechanism would be the opposite of what has been described in great detail in series of papers, for "deactivation" of Au electrodes with $OH^{\cdot}$ generated by the Fenton reagent in mildly acidic medium [23]. In that case, the $OH^{\cdot}$ radicals effectively "polished" the Au electrode, removing asperities that apparently serve as the active centers for electron transfer involving radical formation. Likewise, after the "polishing", the redox behavior of Ru(II)/Ru(III) couple was not affected.

The final steady-state scans of CV curves for AGEs ($N = 2$–7) during propanol oxidation are shown in Fig. 6. The arrows again indicate the increase/decrease of the peak currents. It increases in *n*-PrOH for both peaks from the first to the 20th scan for the even-AGEs, while it decreases for the odd-AGEs. The exception is the slight increase for both peaks observed for AGE-7 in *i*-PrOH. Note also, that the position of the peak again does not change, indicating that the increased value of the peak current reflects only the change in the number of active sites at which the oxidation takes place and not in the change of the electrode kinetics. Thus the behavior of AGE electrodes seems to follow either the activation or the deactivation path, depending on the odd–even number of gold atoms. This behavior is illustrated in greater detail on AGE-4 and AGE-5 respectively, which represents the entire even–odd series. The rate of oxidation of both propanols at AGE-4 increases (Fig. 7a, b) while at the AGE-5 it decreases (Fig. 7c, d). There is also a remarkable difference in the behavior of AGE-5 with respect to *n*-PrOH and *i*-PrOH. Although the absolute values of the current (for peak at −100 mV) are again approximately 20× higher for AGE-4 than for AGE-5, there is a finite oxidation current at the switching potential (+450 mV) (Fig. 7c, d), indicating that for the odd-AGEs there is only a minimal blockage of the electrode at the end of the positive scan. The icons representing the theoretically calculated shapes of the corresponding atomic clusters are included in the individual panels of Fig. 7. Contrary to the reported deactivation of polycrystalline Au in acidic medium [23], the exposure of the AGEs to the Fenton reagent always increased the peak current of AGEs. At the dimensions involved in AGEs, it is hard to argue about "annealing of asperities" being responsible for the "activation" behavior. The observed differences between the odd and even numbered AGEs suggest that the "activation/deactivation" phenomenon is related to the prevailing electronic structure of the active sites.

4 Conclusions

Polycrystalline gold is usually regarded as an "inert" electrode. Experiments described here and confirmed by

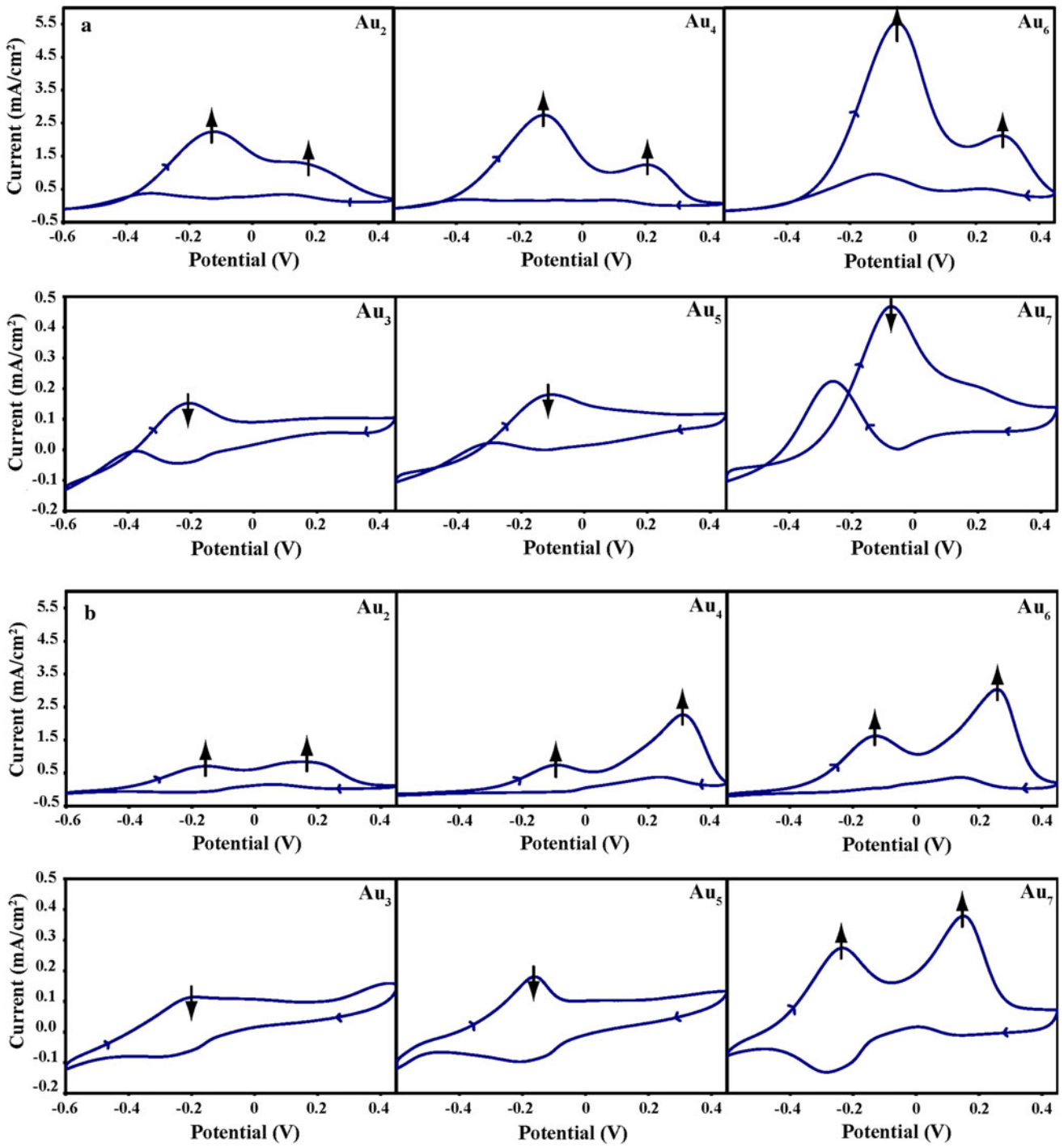

Fig. 6 The survey presentation of the activation pattern for the AGEs ($2 < N < 7$) for **a** n-PrOH and **b** i-PrOH. Only the final CV's are shown and the arrows again indicate the up/down change. The current scales are greater for the even-AGEs in order to facilitate the visual inspection

others indicate that it is anything but "inert". The AGEs described in this paper are truly three-dimensional electrodes in which the Pt substrate, the PANI isolation matrix, and the inserted atomic gold all play an important role. When prepared in atomic format, the AGEs retain most features of bulk gold electrochemistry, but add some significant differences which are related to the odd–even quantum effects predicted for atomic clusters of metals [20, 21].

There is a catalytic effect for oxidation at both odd and even numbered atomic agglomerates of gold that is predicated on the presence of Pt substrate. It is significantly higher for the even-numbered agglomerates. It indicates

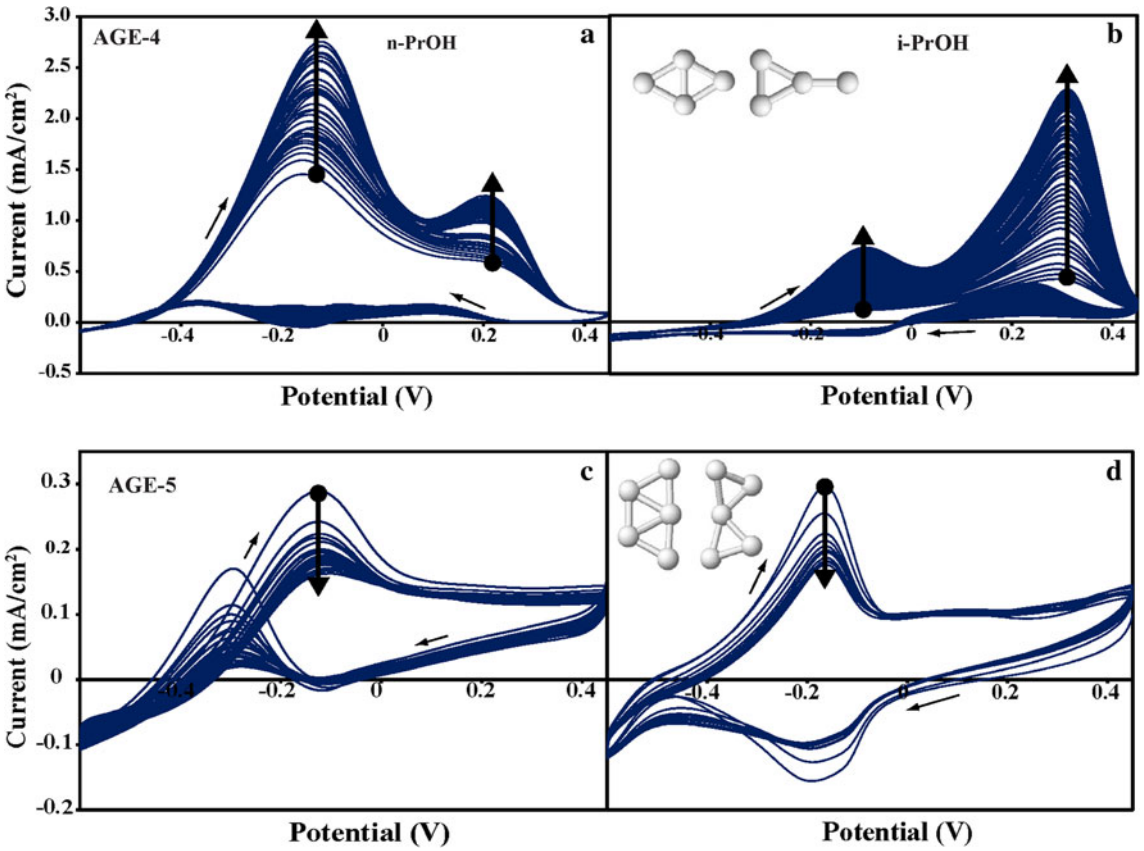

Fig. 7 Comparison of the activation pattern for (*rows*) Pt/PANI/Au_4 and Pt/PANI/Au_5 and for *n*-PrOH and *i*-PROH (*columns*). The differences are discussed in the text. The inserted icons represent the theoretically predicted highest probability shapes of Au clusters [20, 21]

that PANI in alkaline medium is somewhat conducting and porous and that a part of electrochemistry takes place at the Pt surface. The atomic gold acts as a dopant for PANI in the similar way as the anions do for PANI in acidic medium. The Pt surface contributes to the oxygen reduction and generation of the $OH^{\cdot}$ radical. The formed $OH^{\cdot}$ is possibly stabilized by PANI and the ensuing oxidation takes place at atomic gold according to its odd–even pattern. Under these conditions, it is necessary to compare the current efficiency on the basis of active Au atoms, rather than on the usual scale of the geometric area of the electrode. In order to have a rational comparison of performance of AGE with macroscopic polycrystalline gold electrodes, we have arbitrarily chosen 10 μm as the convenient minimum thickness of a thin Au electrode prepared by e.g evaporation, and calculated the number of Au atoms in such an electrode. The estimated amount of Au in AGE of the comparable area and at comparable current efficiency is approximately 3 orders of magnitude lower than for a polycrystalline gold electrode. Besides the major improvement of economy, AGEs offer also possibility of enhanced catalytic selectivity due to the shape-related, quantized odd–even effect.

Acknowledgments This work has been supported by the Georgia Research Alliance.

References

1. Lamy C, Belgsir EM, Leger JM (2001) J Appl Electrochem 31:799
2. Sen Gupta S, Datta J (2005) J Chem Sci 117: 337
3. Kwon Y, Lai SCS, Rodriguez P, Koper MTM (2011) J Am Chem Soc 133:6914
4. Cherevko S, Kulyk N, Chung C-H (2012) Electrochem Acta 69:190
5. de Lima RB, Varela H (2008) Gold Bulletin 41:15
6. Matsuoka K, Inaba M, Iriyama Y, Abe T, Ogumi Z, Matsuoka M (2002) Fuel Cells 2:35
7. Beltowska-Brzezinska M, Luczak T, Holze R (1997) J Appl Electrochem 27:999
8. Smith JA, Josowicz M, Janata J (2003) J Electrochem Soc 150:E384
9. Hatchett DW, Josowicz M (2008) Chem Rev 108:746
10. Genies EM, Boyle A, Lapkowski M, Tsintavis C (1990) Synth Met 36:139
11. Syed AA, Dinesan MK (1991) Talanta 38:815
12. Jonke AP, Josowicz M, Janata J, Engelhard MH (2010) J Electrochem Soc 157:P83
13. Saheb A, Smith JA, Josowicz M, Janata J, Baer DR, Engelhard MH (2008) J Electroanal Chem 621:238

14. Jonke AP, Josowicz M, Janata J (2012) J Electrochem Soc 159:P40
15. McMurry J (2003) Organic chemistry. Brooks/Cole, Belmont
16. Desilvestro J, Weaver MJ (1986) J Electroanal Chem 209:377
17. Celdran R, Gonzalez-Velasco JJ (1981) Electrochem Acta 26:525
18. Ye JQ, Liu HP, Xu CW, Jiang SP, Tong YX (2007) Electrochem Commun 9:2760
19. Ocon P, Alonso C, Celdran R, Gonzalez-Velasco J (1986) J Electroanal Chem 206:179
20. Fernandez EM, Soler JM, Garzon IL, Balbas LC (2004) Phys Rev B 70:
21. Hakkinen H, Landman U (2000) Phys Rev B 62:R2287
22. Bard J, Faulkner RL (2001) Electrochemical methods: fundamentals and applications. Wiley, New York
23. Nowicka AM, Hasse U, Sievers G, Donten M, Stojek Z, Fletcher S, Scholz F (2010) Angewandte Chemie -International Edition, 49: 3006–3009